Evaluation of cellular uptake, cytotoxicity and cellular ultrastructural effects of heteroleptic oxidovanadium(IV) complexes of salicylaldimines and polypyridyl ligands

Gonzalo Scalese [a], Isabel Correia [b], Julio Benítez [a], Santiago Rostán [a], Fernanda Marques [c], Filipa Mendes [c], António Pedro Matos [d], João Costa Pessoa [b,*], Dinorah Gambino [a,*]

[a] Cátedra de Química Inorgánica, Facultad de Química, Universidad de la República, Gral. Flores 2124, 11800, Montevideo, Uruguay
[b] Centro de Química Estrutural, Instituto Superior Técnico, Universidade de Lisboa, Av Rovisco Pais, 1049-001, Lisboa, Portugal
[c] Centro de Ciências e Tecnologias Nucleares, Instituto Superior Técnico, Universidade de Lisboa, Estrada Nacional 10, 2695-066, Bobadela LRS, Portugal
[d] Centro de Investigação Interdisciplinar Egas Moniz, Campus Universitário, Quinta da Granja, Monte de Caparica, Portugal

ARTICLE INFO

ABSTRACT

Searching for prospective vanadium-based drugs for cancer treatment, a new series of structurally related [$V^{IV}O(L-2H)(NN)$] compounds (**1–8**) was developed. They include a double deprotonated salicylaldimine Schiff base ligand (L-2H) and different NN-polypyridyl co-ligands having DNA intercalating capacity. Compounds were characterized in solid state and in solution. EPR spectroscopy suggests that the NN ligands act as bidentate and bind through both nitrogen donor atoms in an axial-equatorial mode. The cytotoxicity was evaluated in human tumoral cells (ovarian A2780, breast MCF7, prostate PC3). The cytotoxic activity was dependent on type of cell and incubation time. At 24 h PC3 cells presented low sensitivity, but at 72 h all complexes showed high cytotoxic activity in all cells. Human kidney HEK293 and ovarian cisplatin resistant A2780cisR cells were also included to evaluate selectivity towards cancer cells and potency to overcome cisplatin resistance, respectively. Most complexes showed no detectable interaction with plasmid DNA, except **2** and **7** which depicted low ability to induce single strand breaks in supercoiled DNA. Based on the overall cytotoxic profile, complexes with 2,2′-bipyridine and 1,10-phenanthroline ligands (**1** and **2**) were selected for further studies, which consisted on cellular distribution and ultrastructural analyses. In the A2780 cells both depicted different distribution profiles; the former accumulates mostly at the membrane and the latter in the cytoskeleton. Morphology of treated cells showed nuclear atypia and membrane alterations, more severe for **1**. Complexes induce different cell death pathways, predominantly necrosis for **1** and apoptosis for **2**. Complexes alternative mode of cell death motivates the possibility for further developments.

1. Introduction

The recognition of the relevance of vanadium in several biological processes has led to increasing research on the potential medicinal uses of its compounds [1,2]. Although traditional research on vanadium medicinal chemistry has been mainly focused on improving biodistribution and tolerability of the vanadium insulin-enhancing moiety or on the development of anti-tumoral compounds, vanadium complexes have also been proposed for the treatment of other diseases, such as those caused by parasites. Nevertheless, no vanadium compound is currently used in the clinical setting [3–8].

Chemo-preventive and anti-tumoral effects of vanadium compounds have been widely investigated on various types of tumor cell lines and on experimental animal models, but the underlying mechanisms of action remain not fully understood. Vanadium compounds have shown ability to disrupt the cellular metabolism through generation of radical oxygen species (ROS) [9], changes in cellular organelles such as lysosomes, mitochondria, and proteins such as actin and tubulin [10–12], and effects on signal transduction pathways, cyclins and caspases, which play a role in cell cycle arrest and apoptosis [13,14]. Additionally, cell proliferation may be also affected via DNA damage [1,15].

Vanadium-*N*-salicylideneamino acidato compounds have attracted the attention of different research groups during decades. They mimic enzymatic systems that involve the formation of a Schiff base by condensation of an aromatic aldehyde (pyridoxal) and an amino acid, with the metal ion promoting the preservation of the planarity of the conjugated system through chelate ring formation [16]. Although, the first objective was to prove the functionality of oxidovanadium(IV/V) *N*-salicylideneamino acidato compounds as models of the reactions catalyzed by pyridoxal-containing enzymes, fostering insight on the mechanisms involved [16,17], ternary compounds, including NN planar

polypyridyl co-ligands, were lately developed as prospective metal-based drugs [8,18,19]. The inclusion of the NN heterocyclic base renders the complexes with the ability to bind DNA through intercalation or surface and/or groove binding [20,21].

Searching for prospective vanadium-based drugs for the treatment of cancer, a new series of eight structurally related heteroleptic [V^{IV}O(L-2H)(NN)] compounds was developed. These include a double deprotonated salicylaldimine ligand (L-2H), derived from glycine and salicylaldehyde or 5-bromo-salicylaldehyde, and different NN-polypyridyl co-ligands having DNA intercalating capacity (Fig. 1). The compounds were characterized in the solid state and in solution.

Moreover, to pursuit our goals on developing prospective candidates as anticancer drugs we further explored the biological activity of the compounds in a set of human tumoral cells and plasmid DNA models. How the compounds are distributed inside the cells, the identification of potential targets and attempts to elucidate the mechanisms of cell death may allow to improve our knowledge of such critical cellular events and, also help to achieve a more rational approach in the design of V anticancer drugs.

2. Materials and methods

2.1. Materials

All common laboratory chemicals were purchased from commercial sources and were used without further purification. Salicylaldimine ligands L (Fig. 1) were synthesized in situ from an equimolar mixture of the corresponding aldehyde and glycine as described below (L1 = 5Brsal-Gly = *N*-5-bromosalicylidene-glycinate; L2 = sal-Gly = *N*-salicylidene-glycinate).

2.2. Syntheses of the oxidovanadium(IV) complexes, [V^{IV}O(L-2H))(NN)], 1–8

The [V^{IV}O(L-2H)(NN)] complexes, where L = 5-bromosalicylaldehyde glycine derivative (L1) or salicylaldehyde glycine derivative (L2) and NN = 2,2′-bipyridine (bipy), 1,10-phenanthroline (phen), 5-amine-1,10-phenanthroline (aminophen), 5,6-epoxy-5,6-dihydro-

Fig. 1. Selected NN polypyridyl co-ligands and molecular structure of the oxidovanadium(IV) complexes with tridentate *N*-salicylidene-glycinato ligands studied in this work (dppz = dipyrido[3,2-*a*: 2′,3′-*c*]phenazine, bipy = 2.2′-bipyridine, phen = 1.10-phenanthroline, aminophen = 5-amine-1,10-phenanthroline, epoxyphen = 5.6-epoxy-5,6-dihydro-1,10-phenanthroline and tdzp = [1,2,5]thiadiazolo[3,4-*f*][1,10]phenanthroline).

1,10-phenanthroline (epoxyphen), dipyrido[3,2-*a*: 2′,3′-*c*]phenazine (dppz) or [1,2,5]thiadiazolo[3,4-*f*][1,10]phenanthroline (tdzp), were synthesized using the following general procedure: 0.50 mmol of glycine (42 mg) and 1.0 mmol of sodium acetate were dissolved in 2 mL of distilled water. 0.50 mmol of 5-Br-salicylaldehyde (100 mg) or salicilaldehyde (61 mg) and 0.50 mmol of NN (78 mg bipy, 98 mg phen, 98 mg aminophen, 98 mg epoxyphen, 141 mg dppz or 120 mg tdzp) were dissolved in 3 mL EtOH (MeOH for dppz). Both solutions were mixed; to this mixture a solution of 0.43 mmol V^{IV}OSO$_4$ (108 mg) in 1 mL H$_2$O was added dropwise. The reaction mixture was stirred at room temperature for 30 min. The orange-brown solids were separated by centrifugation, washed five times with 2 mL portions of H$_2$O and dried under vacuum.

2.2.1. [V^{IV}O(L1 −2H)(bipy)]·2H$_2$O, 1
Yield: 57 mg, 22%. Anal. calc. for C$_{19}$H$_{14}$BrN$_3$O$_4$V·2H$_2$O: C, 44.3; H, 3.5; N, 8.2. Found: C, 44.0; H, 3.6; N, 8.1. Electrospray ionization mass spectra (ESI-MS) (MeOH) m/z [Found (Calcd)]: 157.1 (157.07) (40%) [bipy + H]$^+$; 478.9 (478.96) (20%) (Br isotopic pattern) [M + H]$^+$, 523.7 (522.93) (80%) (Br isotopic pattern) [M + 2Na-H]$^+$. Thermogravimetric analysis (TGA) weight loss below 100 °C [Found (Calcd)]: 3.4, 3.2% (7.0%), two weight losses.

2.2.2. [V^{IV}O(L1-2H)(phen)], 2
Yield: 152 mg, 60%. Anal. calc. for C$_{21}$H$_{14}$BrN$_3$O$_4$V: C, 50.1; H, 2.8; N, 8.3. Found: C, 49.8; H, 2.9; N, 8.3. ESI-MS (MeOH) m/z [Found (Calcd)]: 168.8 (168.33) (42%) (Br isotopic pattern) [M + 3H]$^{3+}$; 181.2 (181.07) (10%) [phen + H]$^+$, 241.6 (241.14) (30%) [phen + isoprop + H]$^+$, 275.8 (275.01) (100%) (Br isotopic patterns) [L1 + NH$_4$]$^+$, 383.0 (383.13) (40%) [2phen + Na]$^+$. TGA: absense of crystallization solvent molecules.

2.2.3. [V^{IV}O(L1-2H)(aminophen)]·2H$_2$O, 3
Yield: 136 mg, 49%. Anal. calc. for C$_{21}$H$_{15}$BrN$_4$O$_4$V·2H$_2$O: C, 45.5; H, 3.5; N, 10.1. Found: C, 45.4; H, 3.6; N, 10.0. ESI-MS (MeOH) m/z [Found (Calcd)]: 196.2 (196.09) (32%) [aminophen + H]$^+$; 336.1 (335.99) (70%) (Br isotopic pattern) [L1 + DMSO + H]$^+$, 519.0 (517.98) (45%) (Br isotopic pattern) [M + H]$^+$, 1034.1 (1034.95) (35%) (Br isotopic pattern) [2 M + H]$^+$. TGA weight loss below 100 °C [Found (Calcd)]: 7.1% (6.5%).

2.2.4. [V^{IV}O(L1-2H)(epoxyphen)]·2½H$_2$O, 4
Yield: 97 mg, 35%. Anal. calc. for C$_{21}$H$_{12}$BrN$_3$O$_5$V·2½ H$_2$O: C, 44.8; H, 3.1; N, 7.5. Found: C, 44.7; H, 3.2; N, 7.4. ESI-MS (MeOH) m/z [Found (Calcd)]: 239.0 (239.02) (35%) [epoxyphen + 2Na-H]$^+$; 333.8 (333.89) (65%) [L1 + 2 K–H]$^+$, 577.0 (577.56) (25%) (Br isotopic pattern) [M + isoprop + H]$^+$. TGA weight loss below 100 °C [Found (Calcd)]: 6.9% (8.0%).

2.2.5. [V^{IV}O(L1-2H)(dppz)]·½H$_2$O, 5
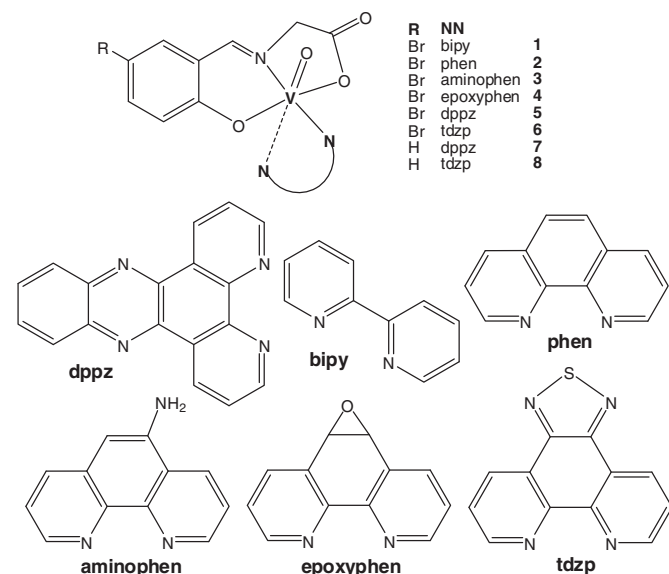Yield: 173 mg, 55%. Anal. calc. for C$_{27}$H$_{17}$BrN$_5$O$_4$V· ½H$_2$O: C, 52.7; H, 2.8; N, 11.4. Found: C, 52.8; H, 2.9; N, 11.4. ESI-MS (MeOH) m/z [Found (Calcd)]: 283.3 (283.09) (45%) [dppz + H]$^+$; 587.0 (587.17) (30%) [2dppz + Na]$^+$. TGA weight loss below 100 °C [Found (Calcd)]: 1.9% (1.5%).

2.2.6. [V^{IV}O(L1-2H)(tdzp)]·2H$_2$O, 6
Yield: 80 mg, 28%. Anal. calc. for C$_{21}$H$_{12}$BrN$_5$O$_4$SV·2H$_2$O: C, 42.2; H, 2.7; N, 11.7; S, 5.4. Found: C, 42.2; H, 2.6; N, 11.6; S, 5.9. ESI-MS (MeOH) m/z [Found (Calcd)]: 168.8 (169.00) (45%) [M + 2H + Na]$^{3+}$; 241.5 (242.00) (35%) [M + 2H]$^{2+}$. TGA weight loss below 100 °C [Found (Calcd)]: 6.0% (6.4%).

2.2.7. [V^{IV}O(L2 −2H)(dppz)]·H$_2$O, 7
Yield: 170 mg, 63%. Anal. calc. for C$_{27}$H$_{17}$N$_5$O$_4$V·H$_2$O: C, 59.6; H, 3.5; N, 12.9. Found: C, 59.5; H, 3.3; N, 12.9. ESI-MS (MeOH) m/z [Found

(Calcd)]: 283.3 (283.02) (50%) $[M + H + K]^{2+}$, 1052.5 (1053.15) (8%) $[2 M + H]^+$. TGA weight loss below 100 °C [Found (Calcd)]: 3.7% (3.3%).

2.2.8. $[V^{IV}O(L2-2H)(tdzp)]\cdot 3H_2O$, 8

Yield: 120 mg, 40%. Anal. calc. for $C_{21}H_{13}N_5O_4SV\cdot 3H_2O$: C, 47.0; H, 3.5; N, 13.1; S, 6.0. Found: C, 47.1; H, 3.4; N, 13.0; S, 5.2. ESI-MS (MeOH): no assignment could be done. TGA weight loss below 100 °C [Found (Calcd)]: 6.1, 4.5% (10.1%), two weight losses.

DMSO solutions of the complexes 1–8 (10^{-3} M) showed molar conductivity (Λ_M) values in the range Λ_M(DMSO): 12.1–13.8 μS/cm^2 and values did not significantly change with time.

2.3. Physicochemical characterization

C, H, N and S analyses were carried out with a Thermo Scientific Flash 2000 elemental analyzer. Thermogravimetric measurements were done with a Shimadzu TGA 50 thermobalance, with a platinum cell, working under flowing nitrogen (50 mL/min) and at a heating rate of 0.5 °C/min (from RT-80 °C) and 1.0 °C/min (from 80 to 350 °C). Conductimetric measurements were done at 25 °C in 10^{-3} M DMSO solutions using a Conductivity Meter 4310 Jenway. Measurements were done over time in order to access the stability of the complexes in this medium. A 500-MS Varian Ion Trap Mass Spectrometer was used to measure ESI-MS spectra of methanolic solutions of the complexes in the positive mode (after dissolution of the complexes in a very small amount of N,N-dimethylformamide (DMF). A combination of several scans was made for each sample.

The Fourier transform infrared spectroscopy (FTIR) absorption spectra (4000–300 cm^{-1}) of the complexes and free ligands were measured as KBr pellets with a Shimadzu IRPrestige-21 instrument. ^{51}V-nuclear magnetic resonance (NMR) spectra of ca. 3 mM solutions of the complexes in DMF (p.a. grade) (5% D$_2$O was added) were recorded on a Bruker Avance III 400 MHz instrument, 24 h after their dissolution. ^{51}V chemical shifts were referenced relative to neat V^{V}OCl$_3$ as external standard. Electron paramagnetic resonance (EPR) spectra were recorded at 77 K with a Bruker ESP 300E X-band spectrometer coupled to a Bruker ER041 X-band frequency meter (9.45 GHz). The complexes were dissolved at room temperature in DMF p.a. grade, previously degassed by passing N$_2$ for 10 min, to obtain ca. 3 mM solutions. The samples were allowed to stand under air at room temperature for 24 h after which ^{51}V NMR (5% D$_2$O was added) and EPR (by keeping the measurement parameters constant) spectra were measured. The 1st derivative EPR spectra of the complexes were normally measured with the samples frozen at 77 K. For some of the complexes samples were also collected for EPR after 4 h under air. The spin Hamiltonian parameters were obtained by simulation of the spectra with a program developed by Rockenbauer and Korecz [22].

2.4. Biological studies

2.4.1. Cells and cell culture

The cell lines A2780/A2780cisR ovarian (Sigma-Aldrich), MCF7 breast, PC3 prostate and HEK293 kidney (ATCC) were grown in culture flasks containing Roswell Park Memorial Institute medium (RPMI) 1640 (ovarian, prostate) or Dulbecco's Modified Eagle Medium (DMEM) + GlutaMAX™-I (breast, kidney) (Gibco) supplemented with 10% Fetal Bovine Serum (FBS) (Gibco) at 37 °C, 5% CO$_2$ in a humidified atmosphere. The cells were adherent in monolayers and when confluent were harvested by digestion with 0.05% trypsin-EDTA (Gibco) and seeded further apart.

2.4.2. Cytotoxicity assays

Stock solutions 10 mM of compounds 1–8 were made in DMSO; then they were diluted in medium to the desired concentrations. For the higher concentration of the compounds in medium (100 μM) the percentage of DMSO is ca. 1%, which at this concentration it has no cytotoxic effect. In the experiments with vanadate(V), Na$_3$VO$_4$ was first diluted in NaOH (1 mM). A stock solution of 20 mM is made; then it was diluted in medium. The maximum concentration was 20 μM. Using this procedure, no decavanadates form. In the experiments with oxidovanadium(IV), the stock solution of V^{IV}OSO$_4$ was prepared by dissolving in water, followed by dilution in water. The required amounts of these solutions were then added to the medium. In this way the precipitation of V^{IV}O(OH)$_2$ is avoided, as well as oxidation of oxidovanadium(IV) before addition to medium.

Cytotoxicity was evaluated with assays based on different modes of detection. MTT (3-(4,5-dimethyl- 2-thiazolyl)-2,5-diphenyl-2H-tetrazolium bromide) assay evaluates the reduction of the tetrazolium salt to insoluble formazan crystals. For the MTT assay cells were grown in 96 well plates and then incubated with the compounds diluted in culture media for different time periods. At the end of the incubation period, the compounds were removed and the cells were incubated with 0.2 mL of MTT solution (0.5 mg/mL phosphate buffered saline (PBS)). After 3 h at 37 °C, 5% CO$_2$, the medium was removed and the purple formazan crystals were dissolved in 0.2 mL of DMSO by shaking. The cellular viability was evaluated by measuring the absorbance at 570 nm [23]. Each experiment was repeated at least twice, and each concentration tested in at least six replicates. The IC$_{50}$ values were calculated from dose-response data (% cellular viability vs. concentration in logarithmic form) using the GraphPad Prism software (version 4.0).

Neutral red (NR = 3-amino-7-dimethylamino-2-methylphenazine hydrochloride) assay evaluates lysosomal integrity and was carried out with a commercial kit (Sigma-Aldrich). After treatment with the complexes, cells were washed with PBS and 0.2 mL serum-free medium containing 0.33% NR was added to each well. The plates were incubated at 37 °C with 5% CO$_2$ for further 3 h. After incubation, the cells were gently rinsed with NR assay fixative, and the incorporated dye was then solubilized in 0.2 mL of NR solubilization agent. The cells were allowed to stand for 10 min. at room temperature in the dark. The cellular viability was evaluated by measuring the absorbance at 540 nm.

Lactate dehydrogenase (LDH) release is as a measure of membrane damage. Following exposure to compounds 1 and 2 for 24 h, 37 °C at 1, 10 and 50 μM concentrations, the culture medium was removed and centrifuged (5000 rpm, 15 min at 4 °C) in order to obtain a cell-free supernatant. The release of LDH in the medium was determined using a commercial kit (BioVision (LDL-cytotoxicity colorimetric assay) following the recommended protocol. The assay utilizes an enzymatic coupling reaction: LDH oxidizes lactate to generate NADH, which then reacts with tetrazolium WST to generate a yellow color solution. The color intensity in each well was measured at 450 nm.

2.4.3. DNA cleavage activity

The plasmid DNA used for gel electrophoresis experiments was PhiX174 (Promega). Linear DNA was obtained by digestion with the single-cutter restriction enzyme XhoI and used as a reference in agarose gel electrophoresis. DNA cleavage activity was evaluated by monitoring the conversion of supercoiled plasmid DNA (Sc — form I) to open circular DNA (Oc — form II) and linear DNA (Lin — form III).

Each reaction mixture was prepared by adding 6 μL of water, 2 μL (200 ng) of supercoiled DNA, 2 μL of 100 mM stock Na$_2$HPO$_4$/HCl pH 7.2 buffer solution and 1 μL of the aqueous solution of the complex. The final reaction volume was 20 μL, the final buffer concentration was 10 mM and the final metal concentration 100 μM. Samples were incubated for 4 and 24 h at 37 °C.

After incubation, 5 μL of DNA loading buffer containing 0.25% bromophenol blue, 0.25% xylene cyanol and 30% glycerol in water (Applichem) were added to each tube and the sample was loaded onto a 0.8% agarose gel in TBE buffer (89 mM Tris–borate, 1 mM EDTA pH 8.3) containing GelRed. Controls of non-incubated and of linearized plasmid were also loaded on each gel. The electrophoresis was carried out for 2 h at 100 V. Bands were visualized under UV light and images captured using an AlphaImagerEP (Alpha Innotech). Peak areas were

measured by densitometry using AlphaView Software (Alpha Innotech). Peak areas were used to calculate the percentage (%) of each form (Sc, Nck and Lin), with a correction factor for the Sc form to account for its lower staining capacity. In each figure all samples were obtained from the same run.

2.4.4. Cellular distribution

The cellular distribution (V content) was evaluated by inductively-coupled plasma mass spectroscopy (ICP-MS) in cellular fractions. Analyses were carried out with a Thermo X-Series Quadrupole ICP-MS instrument (Thermo Scientific) following a previously described method [23]. Briefly, A2780 cells were exposed to complexes **1** and **2** at a concentration equivalent to their IC_{50} at 24 h (10 μM) then washed with cold PBS and centrifuged to obtain the cellular pellet. The cytosol, nucleus, membrane/particulate and cytoskeletal fractions were separated using a commercial kit (FractionPREP cell fractionation kit, BioVision). The content of V in the different fractions were measured after digestion with ultrapure HNO_3 (65%), H_2O_2 and H_3PO_4 in a microwave digestion unit and then diluted in ultrapure water to obtain a solution with 2.0% nitric acid. The instrument was calibrated with a multi-elementar ICP-MS standard solution (Inorganic Venture).

2.4.5. Ultrastructural analysis

Cellular ultrastructural analysis by transmission electron microscopy (TEM) was evaluated with a JEOL 100-SX electron microscope in A2780 cells. Cells at approximately 70% confluence were incubated with compounds **1** and **2** for 24 h at 10 μM. After incubation, cells were treated following a previously described protocol [24,25]. Briefly, after incubation the culture media was replaced by primary fixative consisting of glutaraldehyde (3%) in sodium cacodylate buffer (pH 7.3, 0.1 M) and incubated 2 h at 4 °C. Then the glutaraldehyde solution was discarded and replaced by sodium cacodylate buffer. After 48 h, cells were scraped, pelleted, and embedded in agar (2%) for processing. The cells were then secondarily fixed in osmium tetroxide (1%) in sodium cacodylate, washed in acetate buffer (pH 5.0, 0.1 M) and further fixed in uranyl acetate (0.5%) in acetate buffer. Dehydration was carried out with increasing concentrations of ethanol. The samples were embedded in Epon-Araldite after passage through propylene oxide using SPI-Pon. Thin sections were made with glass or diamond knives and stained with aqueous uranyl acetate (2%) and Reynolds lead citrate. The stained sections were analyzed and photographed.

3. Results and discussion

Eight new ternary $V^{IV}O$-complexes of the salycylaldimines L (L1 = 5Brsal-Gly = N-5-bromosalicylidene-glycinate; L2 = sal-Gly = N-salicylidene-glycinate) and six different NN bidentate co-ligands (Fig. 1) were synthesized in reasonable yields by reaction of $V^{IV}OSO_4$ with stoichiometric amounts of the tridentate ligand L, generated in situ, and the co-ligand. The compounds were characterized in the solid state and in solution using different techniques. Results obtained from elemental analysis, thermogravimetry, conductometry, ESI-MS, FTIR and EPR spectroscopy (described in detail in the following sub-sections) are in agreement with the proposed formulation: $[V^{IV}O(L-2H)(NN)]\cdot xH_2O$. Their molecular formulae are depicted in Fig. 1.

TGA of most complexes showed a weight loss below ca. 100 °C corresponding to the number of water molecules assigned in each case. The compounds **1–8** are non-conducting in DMSO and conductivity did not significantly change with time during at least 3 days [26]. ESI-MS experiments, carried out in the positive mode, confirmed their molecular formulation, as in most cases peaks corresponding to a cation of the [VO(L-2H)(NN)] complex (M), $(M + H^+, M + 2Na-H^+, M + H + K^{2+}$, etc.) were present in the MS-spectra of the compounds. In the case of $[V^{IV}O(L1-2H)(dppz)]$ **7** only peaks corresponding to the dppz ligand could be identified, and for $[V^{IV}O(L1-2H)(tdzp)]$ **8** no assignment

could be made, probably due to the very low solubility of these complexes.

3.1. Characterization of the complexes in the solid state

3.1.1. IR spectroscopic studies

Tentative assignments of the main IR bands were made based on previous reports on vibrational behavior of vanadium complexes of salicylaldimines [17,19,27–29]. Selected bands and their assignment are presented in Table 1.

All complexes show the characteristic strong stretching $\nu(V\!=\!O)$ in the range 950–970 cm^{-1}. The $\nu_{as}(CO_2)$ and $\nu_s(CO_2)$ stretchings appear at ca. 1620–1635 cm^{-1} and 1360–1384 cm^{-1}, respectively. The $\nu(CN)$ appears as a shoulder at around 1600 cm^{-1}. A medium band observed at 1521–1541 cm^{-1}, may originate from the vibration of the (Ph–)C–C($=$N) bond of the salicylaldehyde condensed complexes [17,29]. These results confirm coordination of L by the N_{imine} donor and monodentate CO_2^- coordination [27]. The complexes present a broad band due to presence of water molecules, centered at ~3450–3500 cm^{-1}, and therefore the deprotonation of the salicyladehyde phenol group (OH stretching around 3400 cm^{-1}) could not be established with certainty by analysis of the IR spectra.

3.2. Characterization of the complexes in solution

EPR studies were carried out to further characterize this new series of $V^{IV}O$-complexes. In addition, as the biological activity of the complexes was tested in vitro in aerated diluted solutions and with incubating periods of several days (results in the next sections), additional EPR and ^{51}V NMR spectroscopic studies were carried out to evaluate the stability of the complexes at room temperature towards hydrolysis and/or oxidation of V^{IV}. Most complexes gave orange colored solutions in DMF (except $[V^{IV}O(L1-2H)(bipy)]$, **1**, which was greenish) and no changes in color were observed with time. The DMF solutions were prepared and kept at room temperature, and samples were periodically collected and frozen in liquid nitrogen. Fig. 2 shows the EPR spectra measured for all complexes at 77 K and t = 0. The spin Hamiltonian parameters obtained by simulation are included in Table 2.

All complexes depict axial EPR spectra that exhibit a hyperfine pattern typical of $V^{IV}O$-complexes, consistent with the presence of monomeric $V^{IV}O$-bound species with d^1_{xy} ground-state configuration. Most spectra are compatible with the presence of only one species in solution, but a few show the presence of two coexisting species. This is the case for the complexes derived from L1 that contain bipy (**1**), epoxy (**4**) and dppz (**5**) co-ligands. Previously studied $V^{IV}O$-semicarbazone-bipy complexes also showed the presence of two isomers in solution and higher susceptibility to oxidation [30]. Evaluation of the stability of the compounds over a 24 h period by EPR showed that the bipy complex **1** as well as [VO(L2-2H)(dppz)], **7**, are the least stable. All other complexes present good stability (see Fig. SI-1, Supplementary information), since after 24 h standing in solution under air only a relatively

Table 1
Tentative assignment of selected IR bands of complexes **1–8**. Band positions are given in cm^{-1}.

Compound	$\nu(VO)$	$\nu_{as}(CO_2)$	$\nu_s(CO_2)$	$\nu(Ph-)C-C(=N)$
$[V^{IV}O(L1-2H)(bipy)]$, **1**	959vs	1629vs	1383 m	1526 m
$[V^{IV}O(L1-2H)(phen)]$, **2**	955vs	1628vs	1379 m	1524 m
$[V^{IV}O(L1-2H)(aminophen)]$, **3**	961vs	1629vs	1382 m	1523 m
$[V^{IV}O(L1-2H)(epoxyphen)]$, **4**	954vs	1629vs	1384 m	1535 m
$[V^{IV}O(L1-2H)(dppz)]$, **5**	962vs	1632vs	1379 m	1521 m
$[V^{IV}O(L1-2H)(tdzp)]$, **6**	960vs	1635vs	1380 m	1524 m
$[V^{IV}O(L2-2H)(dppz)]$, **7**	960vs	1633vs	1360 m	1541 m
$[V^{IV}O(L2-2H)(tdzp)]$, **8**	964vs	1620vs	1370 m	1522 m

ν: stretching; vs: very strong, m: medium; L-2H: double deprotonated salicylaldimine ligand, where L1 = 5-bromosalicylaldehyde glycine derivative and L2 = salicylaldehyde glycine derivative.
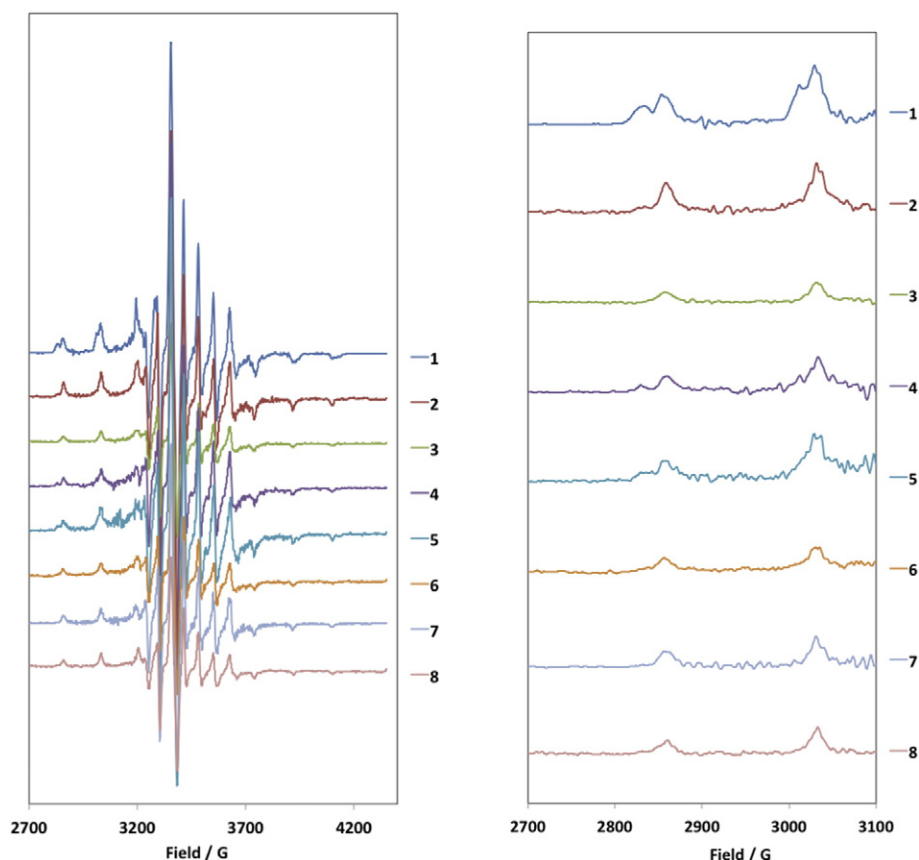
Fig. 2. 1st derivative X-band EPR spectra of frozen solutions of the $V^{IV}O$-complexes in DMF, measured at 77 K.

small decrease is observed in the intensity of the EPR spectra. Fig. 3 shows the spectra measured with time for [VO(L1-2H)(bipy)], **1** and [VO(L1-2H)(aminophen)], **3**.

Table 2 shows the spin Hamiltonian parameters obtained by simulation of the experimental spectra [22]. All studied complexes present comparable values for the spin Hamiltonian parameters, suggesting a similar binding mode for all. As found previously by single-crystal X-ray diffraction for related compounds [19,29,31–34] we expect that the Schiff base ligands are bound to the vanadium center in the equatorial plane forming two chelate rings (6 + 5) through the $O_{phenolato}$, N_{imine} and $O_{carboxylato}$ donors. The N—N ligands are bidentate, one N (here designated as N_{phen}) in the equatorial position and the other *trans* to the O_{oxido} donor. This axial-equatorial binding has been found in other studied mixed-ligand $[V^{IV}O(L)(N—N)]$ complexes with L being a semicarbazone, or a *N*-salicylideneamino acidato, or a dipeptide

ligand, and N—N being bipy, phen, dppz, tzdp, aminophen and epoxyphen [19,28,30–38].

Once a particular binding mode is assumed, for the present set of complexes: {($O_{phenotato}$,N_{imine},$O_{carboxylato}$,N_{phen})$_{equatorial}$ (N_{phen})$_{axial}$}, the values of the hyperfine coupling constant A_z can be estimated (A_z^{est}) using the additivity relationship proposed by Wüthrich [39] and Chasteen [40]: ($A_z^{est} = \Sigma A_{z,i}$ ($i = 1$ to 4), with estimated accuracy of $\pm 3 \times 10^{-4}$ cm^{-1}), where $A_{z,i}$ are the contributions to A_z^{est} of the four equatorially bound ligands. In this work the following values of $A_{z,i}$ were used, for reasons discussed in previous publications [28,30,32,35–38,41–44]: A_z(N_{phen} or N_{bipy}) = 40.4 × 10^{-4} cm^{-1}, A_z($O_{carboxylato}$) = 42.1 × 10^{-4} cm^{-1}, A_z(N_{imine}) = 41.6 × 10^{-4} cm^{-1} and A_z($O_{phenotato}$) = 38.9 × 10^{-4} cm^{-1}. Taking these $A_{z,i}$ values, the A_z^{est} obtained is 163 × 10^{-4} cm^{-1}) which agrees well with those experimentally obtained.

The spin-Hamiltonian parameters of the second species found in the EPR spectrum of [VO(L1-2H)(bipy)] **1** were also obtained, showing a higher A_z value, suggesting solvolysis and substitution of the bipy ligand by DMF. This probably also occurs with the $V^{IV}O$-L1 compounds containing epoxy and dppz ligands, for which a minor secondary species is also present, but whose spin-Hamiltonian parameters were not simulated due to its low intensity.

The evaluation of the stability of the complexes in aerated solutions for a period of 24 h by ^{51}V NMR corroborated the observations made by EPR. The ^{51}V NMR spectra measured after 24 h for all complexes (see Fig. 4) all showed the presence of a relatively weak peak with chemical shifts (δ_V) of ca. −530 ppm, confirming the partial oxidation of V^{IV} to V^V.

We have previously reported on $V^{IV}O$-semicarbazone $V^{IV}O(L)(NN)$ mixed-ligand complexes, also containing phen, bipy, dppz, aminophen, epoxyphen or tzdp as co-ligands, which upon standing in air showed the presence of ^{51}V NMR peaks due to $V^VO_2(L)$ species in the δ_V range ca. −500 to −560 ppm [30,35–38,45–49]. Theoretical calculations carried out predicted the resonance for such V^VO_2-semicarbazone complexes at δ_V values between −515 and −540 ppm [47,50]. For V^V-*o*-

Table 2
Spin Hamiltonian parameters obtained by simulation of the EPR spectra in DMF measured at 77 K.

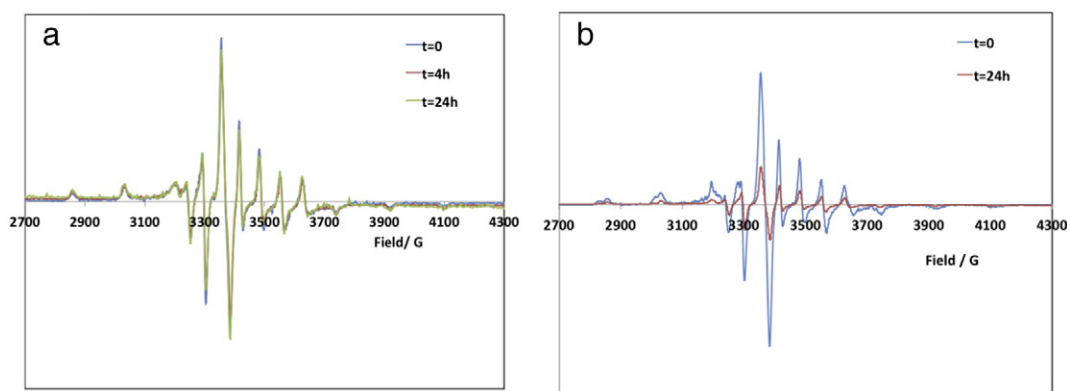| Compound	g_x,g_y	g_z	A_x,A_y ($\times 10^4$ cm^{-1})	A_z ($\times 10^4$ cm^{-1})
$[V^{IV}O(L1\text{-}2H)(bipy)]$, **1**	1.987	1.956	57.7	163.2
	1.987	1.956	58.7	169.0
$[V^{IV}O(L1\text{-}2H)(phen)]$, **2**	1.987	1.955	57.3	162.3
$[V^{IV}O(L1\text{-}2H)(aminophen)]$, **3**	1.987	1.955	58.1	162.5
$[V^{IV}O(L1\text{-}2H)(epoxyphen)]$, **4**	1.988	1.956	57.5	161.6
$[V^{IV}O(L1\text{-}2H)(dppz)]$, **5**	1.988	1.956	58.0	162.6
$[V^{IV}O(L1\text{-}2H)(tdzp)]$, **6**	1.987	1.956	58.3	162.4
$[V^{IV}O(L2\text{-}2H)(dppz)]$, **7**	1.988	1.956	57.8	163.3
$[V^{IV}O(L2\text{-}2H)(tdzp)]$, **8**	1.987	1.956	58.2	161.8

Fig. 3. X-band EPR spectra measured with time for complexes [$V^{IV}O(L1-2H)(aminophen)$], **3** (left) and [$V^{IV}O(L1-2H)(bipy)$], **1** (right).

vanilideneamino acidato complexes (with Ser, Thr, Tyr) in MeOH, δ_V values between −535 and −560 ppm were reported [51], while for V^V-N-salicylideneamino acidato and V^V-N-pyridoxylideneamino acidato complexes (with L-Tyr and o-tyrosine) in water, δ_V values

Fig. 4. ^{51}V NMR spectra measured for solutions (concentrations between 1.1 and 3.2 mM) of the complexes in DMF after 24 h under air.

between −522 and −534 ppm were obtained [52]. Therefore, for the present systems, it is reasonable to conclude that the resonances at ca. −530 ppm, obtained after partial oxidation of complexes **1**–**8** under air, can be assigned to the formation of small amounts of $V^VO_2(L-2H)$ complexes, thus no longer containing the NN co-ligands.

Overall, the spectroscopic and conductometric data obtained with solutions of the $V^{IV}O$-complexes under air showed that most complexes **2**–**8** are reasonably stable to hydrolysis and oxidation, and that in the $V^{IV}O$-complexes the NN heteroligands remain bound in an axial-equatorial mode.
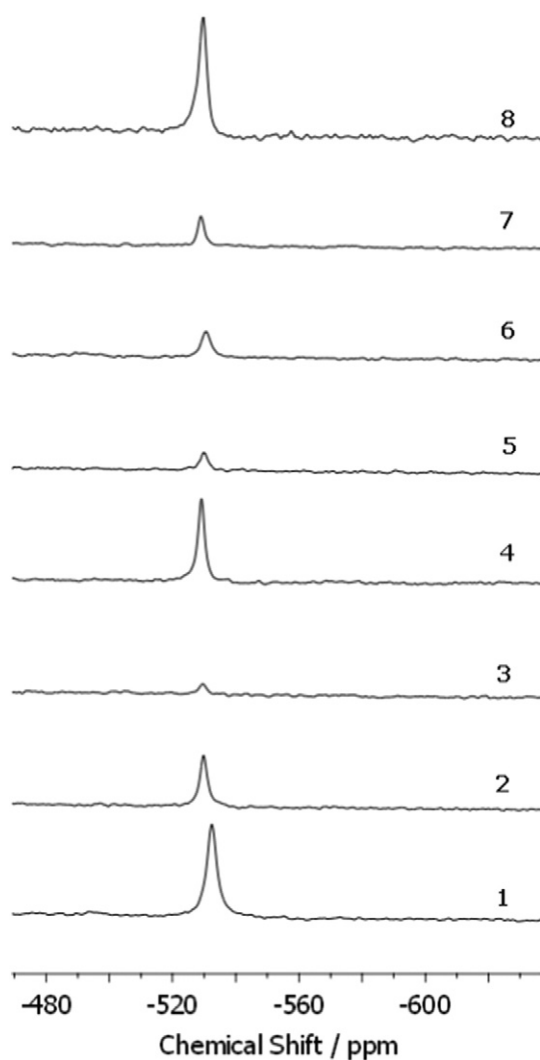
3.3. Biological evaluation

3.3.1. Cytotoxicity studies

The assays used to evaluate the cytotoxic activity are based on different physiological endpoints: the MTT assay is a measure of the metabolic activity of living cells based on the activity of a mitochondria dehydrogenase; and the NR assay is based on the incorporation and binding of neutral red, a weak cationic dye, in the lysosomes of viable cells. Accordingly, cellular viability determined by the NR assay is a measure of lysosomal integrity [53,54].

The MTT assay was carried out for the whole set of cell lines and complexes (**1**–**8**) and the neutral red (NR) assay for the entire series of complexes (**1**–**8**) for the A2780 cells.

The cytotoxicity (IC_{50} values) of complexes **1**–**8** on the human A2780 ovarian, MCF7 breast and PC3 prostate cells at 24 and 72 h incubation by the MTT assay are depicted in Table 3 and Fig. 5. The activity of the complexes is dependent on the type of cancer cell and time of incubation. In the A2780 cells the ligands do not show cytotoxic effect at 24 h but at 72 h, aminophen presented a cytotoxic activity ($IC_{50} = 2.6 \pm 0.9$ μM) similar to its corresponding complex (**3**).

With exception of paired complexes **6**/**8** and **5**/**7**, the bromosalicylaldehyde derivatives were in general more active than their corresponding salicylaldehyde derivatives [19]. In addition, all complexes are in general more cytotoxic than cisplatin for the A2780, MCF7 and PC3 cancer cells at 24 and 72 h challenge. This is a relevant finding considering that these cell lines are representative of the most common human cancer diseases.

The activity of complexes **1**–**8** was also assessed with the MTT assay in the ovarian cisplatin resistant A2780cisR cells to evaluate the ability to overcome cisplatin resistance, as cisplatin is the most important metal-based compound clinically approved. The non-tumoral cell line HEK293 was also included to evaluate the selectivity of the complexes for tumoral cells. Results presented in Table 3 show that the complexes are able to overcome cisplatin resistance. The IC_{50} of cisplatin in the A2780cisR cells after 24 h treatment is much higher than the IC_{50}

Table 3

IC$_{50}$ values of complexes **1–8** on the human tumoral and non-tumoral cell lines at 24 and 72 h incubation, measured by the MTT assay.

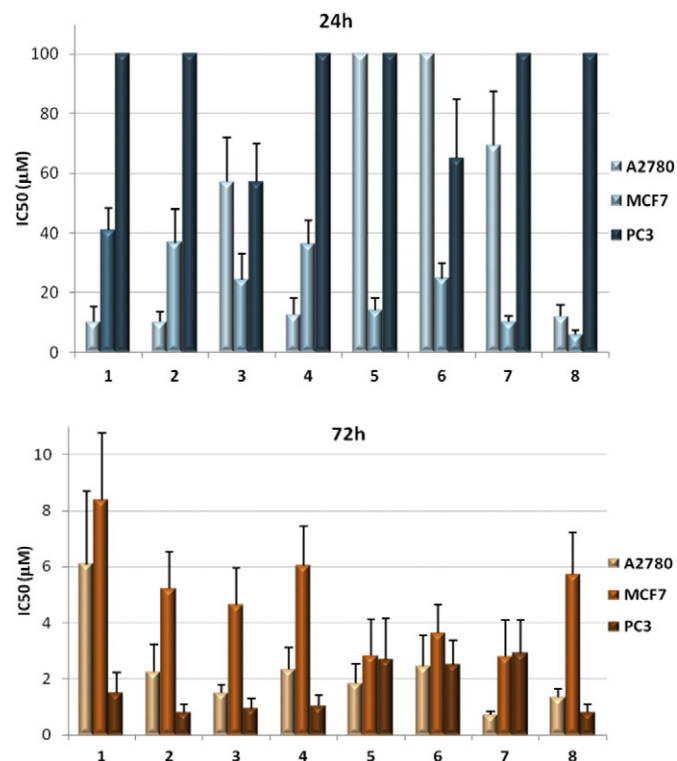| Compounds	IC$_{50}$ (µM), 24 h incubation				
	MCF7 breast	A2780 ovarian	A2780cisR ovarian	PC3 prostate	HEK embryonic kidney
1	40.9 ± 7.5	10.2 ± 5.05	62.9 ± 17	>100	82.8 ± 47.5
2	36.8 ± 11.2	10.3 ± 3.35	89.3 ± 24	>100	28.8 ± 7.2
3	24.3 ± 8.85	86.1 ± 30.5	42.5 ± 22	57.1 ± 23.5	17.0 ± 5.4
4	36.3 ± 8.0	12.6 ± 5.90	40.1 ± 23	109 ± 46	38.1 ± 15.8
5	14.2 ± 3.95	>100	20.6 ± 11	>100	27.9 ± 81
6	24.8 ± 5.15	>100	28.0 ± 13	64.5 ± 2.0	20.0 ± 7.8
7	10.4 ± 1.70	69.4 ± 18.5	13.5 ± 4.2	>100	24.0 ± 8.7
8	5.90 ± 1.45	12.2 ± 3.85	66.2 ± 22	>100	28.5 ± 10.3
Cisplatin	59 ± 12	36 ± 8.0[a]	140 ± 40 [a]	>100	–

Compounds	IC$_{50}$ (µM), 72 h treatment			
	A2780 ovarian	MCF7 breast	PC3 prostate	HEK embryonic kidney
1	6.08 ± 2.67	8.37 ± 2.40	1.50 ± 0.73	30.2 ± 16.6
2	2.25 ± 0.96	5.22 ± 1.3	0.82 ± 0.29	2.24 ± 1.05
3	1.49 ± 0.33	4.66 ± 1.35	0.94 ± 0.35	–
4	2.33 ± 0.79	6.04 ± 1.4	1.05 ± 0.37	–
5	1.85 ± 0.71	2.84 ± 1.27	2.69 ± 1.48	–
6	2.45 ± 1.11	3.64 ± 1.03	2.52 ± 0.85	–
7	0.73 ± 0.13	2.79 ± 1.32	2.92 ± 1.17	–
8	1.35 ± 0.34	5.72 ± 1.51	0.82 ± 0.29	–
Cisplatin	1.9 ± 0.1[a]	28 ± 6.0 [a]	51 ± 7.0	–

[a] [17].
[a] [55,56].

found for the complexes in the A2780 cells at 24 h treatment. Among all complexes, **1** and **2** present higher selectivity for the ovarian cancer cells.

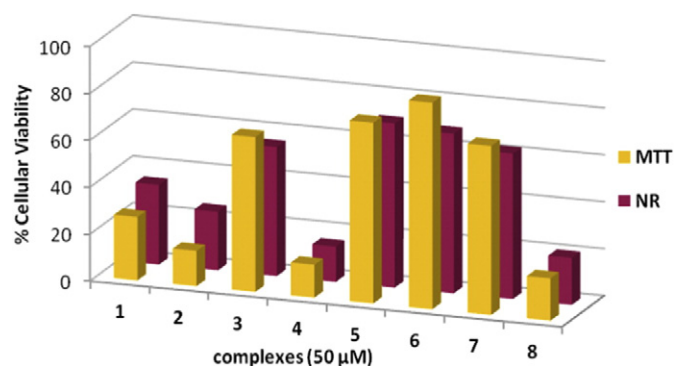The activity of complexes **1–8** in the ovarian cells was also evaluated by the NR assay. Although the assays are based on different principles, they do not differ in sensitivity for all complexes studied at an equimolar concentration (50 µM) (Fig. 6).

Additionally, the cellular toxicity induced by complexes **1** and **2** in the A2780 cells was also assessed by the lactate dehydrogenase (LDH) assay. This assay measures the interconversion of pyruvate and lactate with concomitant interconversion of NADH and NAD$^+$ by the enzyme LDH. Cells rapidly release LDH into the cell culture medium upon damage of the cell membrane. Although complexes **1** and **2** present a similar IC$_{50}$ in the ovarian cells at 24 h treatment, they showed a different LDH release profile. As shown in Fig. 7 the LDH release is dose - dependent and more important for compound **1**.

3.3.2. Species responsible for the biological activity

V^{IV}O-solutions containing bipy or phenanthroline derivatives are reasonably stable to hydrolysis and to oxidation, but is unavoidable that, upon dissolution, the present [V^{IV}O(L-2H)(NN)] complexes partly hydrolyse to [V^{IV}O(L-2H)] and [V^{IV}O(NN)] species, and with time there might be some oxidation of V^{IV} to V^V. The compounds may also decompose into vanadate and V^{IV}O^{2+} thus yielding V^{IV}O-hydrolytic

Fig. 5. IC$_{50}$ values found for complexes **1–8** in the ovarian, breast and prostate cancer cells (24 and 72 h incubation at 37 °C).

Fig. 6. Comparison of the activity of complexes **1–8** in the ovarian cells by the MTT and NR assays (24 h incubation at 50 µM).
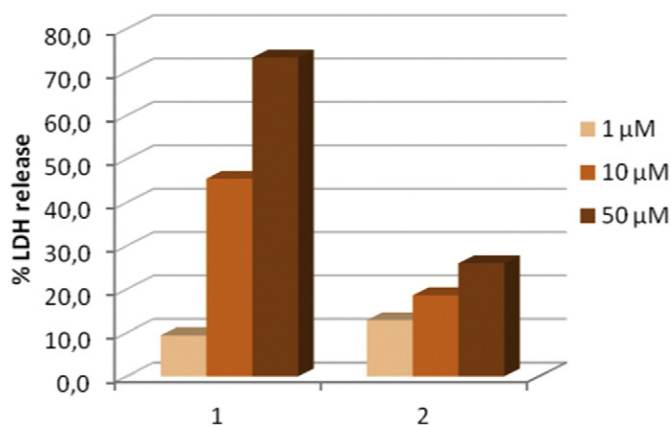
Fig. 7. LDH release from A2780 cells after incubation at 37 °C with **1** and **2** at 1, 10 and 50 μM concentration of complexes.

species. Therefore, the observed biological activity might partly also be due to one of these vanadium-containing species.

The $V^{IV}O$-Schiff base complexes, $[V^{IV}O(L-2H)]$, are not stable in aqueous buffered solutions [6,17,19], so we anticipate they are not relevant regarding the cytotoxicity observed. On the other hand, the V^{V}-Schiff base complexes, $V^{V}O_2(L-2H)$ complexes, were detected in small amounts (Fig. 4). However, not many of such complexes have been properly characterized in the solid state [16], and to our knowledge no previous cytotoxicity study was published for this type of compounds; therefore, we cannot predict their contribution to the activity measured.

Concerning possible contribution of vanadate to the cytotoxicity, above we discussed the characterization of the systems by ^{51}V NMR spectra. However, in these experiments we did not detect V^{V}-aquo species; if these form it will be in low concentrations. In previous cell viability studies with HeLa and 3 T3-L1 fibroplats cells incubated with vanadate, the IC_{50} at 72 h for vanadate was ~32 μM (HeLa cells) and ~36 μM (3 T3-L1 fibroplats), significantly higher values than those obtained here for the $[V^{IV}O(L-2H)(NN)]$ complexes [57]. Yet, at shorter incubation times with HeLa cells (24 h, 37 °C) no important cytotoxicity was observed at high vanadate concentrations ($IC_{50} > 200$ μM) (data not shown). Therefore, as the amount of vanadate present should be low in our incubating solutions, we do think its effect is not relevant in our studies.

Concerning possible contribution to the cytotoxicity of $V^{IV}O$-aquo species in the incubating solutions, there are previous studies describing biological effects carried out with solutions containing $V^{IV}OSO_4$. However, these data should be interpreted with care. Indeed, it is known that oxidovanadium(IV) - $V^{IV}O^{2+}$ — extensively hydrolyzes in aqueous solution [16,58] and above ca. 50–100 μM concentration, the $VO(OH)_2$ precipitates in the pH range 4–7. Additionally it will oxidize to V(V) at pH > 4, and that will certainly occur fast, particularly at low total vanadium concentration, if $V^{IV}O^{2+}$ is not bound to a suitable ligand. Therefore, $V^{IV}O^{2+}$ will not exist as such at pH ~7, the relative amount of the

predominant species, mainly $[(V^{IV}O)_2(OH)_5^-]_n$ and $V^{IV}O(OH)_3^-$, depending on the total vanadium(IV) concentration [16,58].

Notwithstanding, several in vitro studies reporting biological effects of $V^{IV}OSO_4$ have been reported [59–63]. In some cases, the authors simply state that biological effects were observed, as well as cell survival studies, with no measure of IC_{50} values, in most cases because these would be higher than ca. 100 μM. In other cases IC_{50} values are reported, normally either at 24 or 48 h incubation periods, range from 19.4 ± 2.0 μM (MDA-MB468 breast cancer cell line) to 49.0 ± 2.5 μM (SKBR3 breast cancer cell line), 95.7 ± 4.8 μM (MDA-MB231 breast cancer cell line) and >100 μM (T47D breast cancer cell line) [59]. Considering the comments above regarding oxidovanadium(IV) solutions, we would expect these biological effects to be due both to vanadate(V) and $V^{IV}O$-species present in the incubation solutions.

To confirm a possible effect of $Na_3V^{V}O_4$ and $V^{IV}OSO_4$ additional studies were carried out in this work incubating these compounds at concentrations within the range 0.1–200 μM with the A2780 cells during 24 h. The results show that both compounds had no important activity against the ovarian cells (see Fig. SI-2, Supplementary information). The IC_{50} values found are 156 ± 20 μM and 254 ± 27 μM for $Na_3V^{V}O_4$ and $V^{IV}OSO_4$, respectively.

Overall we would consider the cytotoxicity of the present compounds as mainly due to either $[V^{IV}O(L-2H)(NN)]$ or $[V^{IV}O(NN)]$ complexes interacting with cells. The exact species acting inside cells and mechanism of action remain to be elucidated, the following sections providing some relevant information.

3.3.3. DNA cleavage evaluation

To assess the DNA cleavage ability of the vanadium complexes, supercoiled φX174 phage DNA was incubated with the compounds at 100 μM, in phosphate buffer (pH 7.2) for two different periods: short (4 h) and long (24 h) at 37 °C.

The DNA cleavage activity was evaluated by monitoring the conversion of supercoiled plasmid DNA (Sc – form I) to open circular DNA (Oc-form II) and linear DNA (Lin –form III). The naturally occurring supercoiled form (Form I), when nicked, gives rise to an open circular relaxed form (Form II) and upon further cleavage, results in the linear form (Form III). When subjected to gel electrophoresis, relatively fast migration is observed for Form I, form II migrates slowly and Form III migrates between Forms I and II. The distribution of the three DNA forms in the agarose gel electrophoresis provides a measure of the extent of DNA cleavage.

Fig. 8 shows the electrophoretic pattern of plasmid DNA incubated with complexes **1–8**, for the two incubation periods tested, as well as the control samples.

From the gel electrophoresis analysis it is possible to conclude that after 4 h there is no alteration of the mobility of DNA isoforms. After 24 h it can be observed that most of the V complexes were not able to induce conformational changes in DNA, when compared with the DNA control (incubated in the same conditions, in the absence of any metal complex).
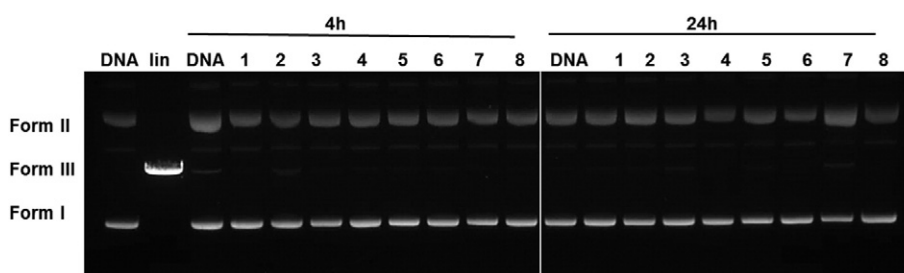
Fig. 8. Interaction of plasmid DNA with complexes **1–8** (100 μM) after 4 or 24 h of incubation at 37 °C in phosphate buffer (pH 7.2). Forms I, II and III are supercoiled, open circular and linear forms of DNA, respectively. DNA lin - linear DNA was obtained by digestion with single-cutter restriction enzyme *Xho*I. Data are a representative from three independent experiments.
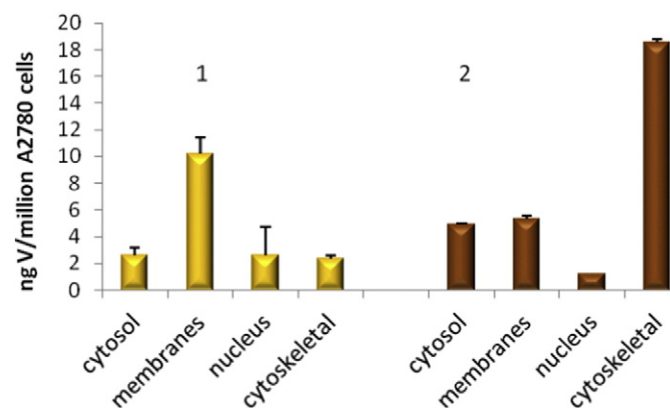
Fig. 9. Vanadium accumulation (ng/10^6 cells) in the A2780 subcellular fractions. Cells were exposed to complexes **1** and **2** at a concentration of 10 μM, equivalent to their IC$_{50}$ at 24 h. Data are mean (SD) of two independent experiments.

Only the samples incubated with compounds **2** and **7** show a slight conformational change in DNA. The interaction of these two complexes with DNA gives rise to a slightly higher proportion of circular form (Form II), but with no linear form detected (Form I), which points out for the occurrence of single-strand breaks without significant formation of double-strand breaks.

The supercoiled/circular (Sc/Oc) ratio calculated for the samples incubated with compounds **2** and **7** are approximately 20 and 40% smaller than that of the control (without addition of any vanadium complex). For the remaining compounds the Sc/Oc ratio found is similar to that obtained for the control DNA. Overall, the V complexes depict no or very low DNA-cleavage activity.

3.3.4. Subcellular distribution

The subcellular distribution of complexes **1** and **2** in A2780 cells was evaluated by ICP-MS in cellular fractions prepared by fractionation. The V content was determined after 24 h treatment with the complexes at a concentration equivalent to their IC$_{50}$ (10 μM). Results presented in Fig. 9 show that the V content present a different distribution profile in the cells incubated with the complexes; for **1** the total amount of V up-taken is lower than for complex **2** (17.8 vs 29.9 ng V/10^6 cells). Moreover, for **1** about 60% of V taken by the cells accumulated in the membrane/particulate fraction, while for **2** about 60% is retained in cytoskeletal fraction. For both complexes the uptake in the nucleus is small, in particular for compound **2** (only 4% total uptake). This result indicates that compounds can target different cellular components, and that DNA is probably not the main target.

3.3.5. Ultrastructural analysis

The ultrastructure analysis by TEM can give an indication of cellular damage and site of action and also provides insights on the underlying mechanisms of action. Thus, TEM was used to investigate the effects of compounds **1** and **2** on the morphologic alterations of A2780 cells. Representative images obtained for both compounds are depicted in Fig. 10. The results revealed that after treatment with both compounds at a concentration equivalent to their IC$_{50}$ (10 μM, 24 h); the cells presented membrane alterations, nuclear atypia and mitochondria densification that were absent in controls (cells with no treatment). Moreover, the compounds induced spindle shaped cytoplasmic clefts that could have intimate relation with the membrane alterations observed [64–66]. Occasionally, intermediate filaments (vimentin) also accumulate in cells treated with the vanadium complexes. These filaments are structural components of the cytoskeleton that play important roles in cellular biological functions [67,68]. Apoptotic cells were found in cultures treated with compound **2**, in contrast with compound **1** which showed predominantly necrotic cells and severe membrane damage.

4. Conclusions

A new series of structurally related mixed-ligand complexes, [V^{IV}O(L-2H)(NN)], was synthesized where L are *N*-salicylideneglycinate Schiff bases and NN are several distinct polypyridyl co-ligands having DNA intercalating capability. The compounds were characterized in
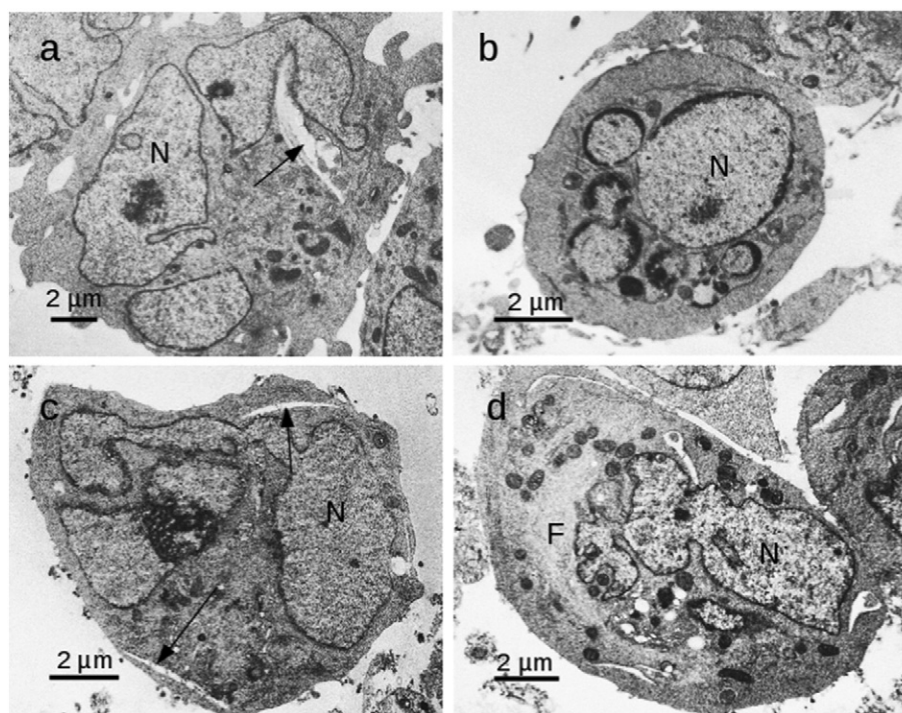
Fig. 10. TEM images showing the ultrastructure of A2780 cells after treatment with vanadium complexes **1** and **2** (10 μM, 24 h); (a) and (b) – compound **2**; (c) and (d) compound **1**. Results showed highly convoluted and deeply indented nucleus for both compounds (N) as well as cytoplasmic clefts (arrows); Apoptotic cells are found in cells treated with compound **2** (b); Cytoplasmic filament bundles were found in cells treated with compound **1** and to a lesser extent compound **2** (d).

the solid state and in solution. EPR spectroscopy indicates that the binding set corresponds to $O_{phenotato}$, N_{imine}, $O_{carboxylato}$ and one of the N_{phen} bound equatorially, and another N_{phen} bound axially. Thus, NN co-ligands act as bidentate in an axial-equatorial mode, as found previously for several previously characterized related $V^{IV}O$-complexes. EPR and ^{51}V NMR spectroscopy carried out with aerated solutions indicate that the compounds are reasonably stable to hydrolysis and oxidation up to 24 h, most of them yielding relatively small amounts of $V^VO_2(L-2H)$.

Vanadium compounds have been reported to induce alterations in cellular organelles such as lysosomes, mitochondria, and cytoskeleton proteins such as actin and tubulin, as well as to produce effects on signal transduction pathways, cell cycle arrest and induction of apoptosis. Some of these effects may be mediated through DNA damage. This study revealed interesting findings with these structurally related $V^{IV}O$-complexes containing polypyridyl based co-ligands. The effects observed e.g., cytotoxicity, morphological alterations (membrane and nuclear) seem not to be mediated by DNA damage, as only complexes **2** and **7** show some (very low) DNA-cleavage activity and slight occurrence of single-strand damage.

Although vanadium complexes **1** and **2** displayed similar cytotoxic activity in the ovarian cells after 24 h incubation, their cellular uptake profiles are quite different, as well as their cellular effects. In fact, for compound **1** the higher accumulation in the membrane resulted in more membrane damage, as could be seen by higher percentage of LDH release compared to compound **2**.

Moreover, the cellular effects observed by TEM seemed more severe for complex **1**, containing the bipyridine co-ligand, than for compound **2**, containing phenanthroline. In common for both compounds, the mechanism of action seems to be related with the disruption of the endomembranar system and marked alterations of the nuclear profile, which was more severe for compound **1**. Noteworthy, the IC_{50} values at 24 h for the HEK embryonic kidney cells are higher for compound **1** than for **2–8**, and much higher at 72 h in comparison with **2**, thus indicating significantly superior selectivity of the vanadium complex **1**, particularly for the A2780 cells.

The global results point at this new series of oxidovanadium(IV) compounds as promising compounds to be further explored in the development of more effective and less toxic anticancer drugs.

Acknowledgements

Appendix A. Supplementary data

Supplementary data to this article can be found online at http://dx.doi.org/10.1016/j.jinorgbio.2016.11.010.

References

[1] J. Costa Pessoa, S. Etcheverry, D. Gambino, Coord. Chem. Rev. 301-302 (2015) 24–48.
[2] D. Rehder, Biological activities of V and Cr, in: J. Reedijk, K. Poeppelmeier (Eds.), Comprehensive Inorganic Chemistry II, vol. 3, Elsevier, Oxford 2013, pp. 819–834.
[3] D. Rehder, Dalton Trans. 42 (2013) 11749–11761.
[4] J. Costa Pessoa, I. Tomaz, Curr. Med. Chem. 17 (2010) 3701–3738.
[5] G.R. Willsky, L.H. Chi, M. Godzala, P.J. Kostyniak, J.J. Smee, A.M. Trujillo, J.A. Alfano, W.J. Ding, Z.H. Hu, D.C. Crans, Coord. Chem. Rev. 255 (2011) 2258–2269.
[6] D. Rehder, Future Med. Chem. 4 (2012) 1823–1837.
[7] D. Rehder, 2014. in: A. Sigel, et al., (Eds.), Interrelations between Essential Metal Ions and Human Diseases, Metal Ions in Life Sciences, 13, © Springer Science + Business Media, Dordrecht, 2014, http://dx.doi.org/10.1007/978-94-007-7500-8_5.
[8] D. Gambino, Coord. Chem. Rev. 255 (2011) 2193–2203.
[9] I.E. León, A.L. Di Virgilio, V. Porro, C.I. Muglia, L.G. Naso, P.A. Williams, M. Bollati-Fogolin, S.B. Etcheverry, Dalton Trans. 42 (2013) 11868–11880.
[10] J. Rivadeneira, D.A. Barrio, G. Arrambide, D. Gambino, L. Bruzzone, S.B. Etcheverry, J. Inorg. Biochem. 103 (2009) 633–642.
[11] C. Yuan, L. Lu, X. Gao, Y. Wu, M. Guo, Y. Li, X. Fu, M. Zhu, J. Biol. Inorg. Chem. 14 (2009) 841–851.
[12] Y. Zhao, L. Ye, H. Liu, Q. Xia, Y. Zhang, X. Yang, K. Wang, J. Inorg. Biochem. 104 (2010) 371–378.
[13] I.E. León, P. Díez, S.B. Etcheverry, M. Fuentes, Metallomics 8 (2016) 739–749.
[14] Y. Fu, Q. Wang, X.G. Yang, X.D. Yang, K. Wang, J. Biol. Inorg. Chem. 13 (2008) 1001–1009.
[15] I.E. León, N. Butenko, A.L. Di Virgilio, C.I. Muglia, E.J. Baran, I. Cavaco, S.B. Etcheverry, J. Inorg. Biochem. 134 (2014) 106–117.
[16] J. Costa Pessoa, J. Inorg. Biochem. 147 (2015) 4–24.
[17] J. Costa Pessoa, M.J. Calhorda, I. Cavaco, P.J. Costa, I. Correia, D. Costa, L.F. Vilas-Boas, V. Felix, R.D. Gillard, R.T. Henriques, R. Wiggins, Dalton Trans. (2004) 2855–2866.
[18] U. Saha, T.K. Si, P.K. Nandi, K.K. Mukherjea, Inorg. Chem. Commun. 38 (2013) 43–46.
[19] I. Correia, S. Roy, C.P. Matos, S. Borovic, N. Butenko, I. Cavaco, F. Marques, J. Lorenzo, A. Rodríguez, V. Moreno, J. Costa Pessoa, J. Inorg. Biochem. 147 (2015) 134–146.
[20] P.K. Sasmal, A.K. Patra, M. Nethaji, A.R. Chakravarty, Inorg. Chem. 46 (2007) 11112–11121.
[21] G. Scalese, J. Benítez, S. Rostán, I. Correia, L. Bradford, M. Vieites, L. Minini, A. Merlino, E.L. Coitiño, E. Birriel, J. Varela, H. Cerecetto, M. González, J. Costa Pessoa, D. Gambino, J. Inorg. Biochem. 147 (2015) 116–125.
[22] A. Rockenbauer, L. Korecz, Appl. Magn. Reson. 10 (1996) 29–43.
[23] L. Côrte-Real, F. Mendes, J. Coimbra, T.S. Morais, A.I. Tomaz, A. Valente, M.H. Garcia, I. Santos, M. Bicho, F. Marques, J. Biol. Inorg. Chem. 19 (2014) 853–867.
[24] S. Gama, F. Mendes, F. Esteves, F. Marques, A. Matos, J. Rino, J. Coimbra, M. Ravera, E. Gabano, I. Santos, A. Paulo, Chembiochem 13 (2012) 2352–2362.
[25] L. Côrte-Real, A.P. Matos, I. Alho, T.S. Morais, A.I. Tomaz, M.H. Garcia, I. Santos, M.P. Bicho, F. Marques, Microsc. Microanal. 19 (2013) 1122–1130.
[26] W.J. Geary, Coord. Chem. Rev. 7 (1971) 81–91.
[27] K. Nakamoto, Infrared and Raman Spectra of Inorganic Compounds, fifth ed. Wiley, 1997.
[28] J. Costa Pessoa, I. Cavaco, I. Correia, M.T. Duarte, R.D. Gillard, R.T. Henriques, F.J. Higes, C. Madeira, I. Tomaz, Inorg. Chim. Acta 293 (1999) 1–11.
[29] J. Costa Pessoa, M.J. Calhorda, I. Cavaco, I. Correia, M.T. Duarte, V. Felix, R.T. Henriques, M.F.M. Piedade, I. Tomaz, J. Chem. Soc. Dalton Trans. (2002) 4407–4415.
[30] M. Fernández, L. Becco, I. Correia, J. Benítez, O.E. Piro, G.A. Echeverria, A. Medeiros, M. Comini, M.L. Lavaggi, M. González, H. Cerecetto, V. Moreno, J. Costa Pessoa, B. Garat, D. Gambino, J. Inorg. Biochem. 127 (2013) 150–160.
[31] I. Cavaco, J. Costa Pessoa, D. Costa, M.T.L. Duarte, R.D. Gillard, P.M. Matias, J. Chem. Soc. Dalton Trans. (1994) 149–157.
[32] I. Cavaco, J. Costa Pessoa, M.T. Duarte, R.T. Henriques, P.M. Matias, R.D. Gillard, J. Chem. Soc. Dalton Trans. (1996) 1989–1996.
[33] A.J. Tasiopoulos, E.J. Tolis, J.M. Tsangaris, A. Evangelou, J.D. Woollins, A.M. Slawin, J. Costa Pessoa, I. Correia, T.A. Kabanos, J. Biol. Inorg. Chem. 7 (2002) 363–374.
[34] P.K. Sasmal, A.K. Patra, M. Nethaji, A.R. Chakravarty, Inorg. Chem. 46 (2007) 11112–11121.
[35] J. Benítez, L. Guggeri, I. Tomaz, G. Arrambide, M. Navarro, J. Costa Pessoa, B. Garat, D. Gambino, J. Inorg. Biochem. 103 (2009) 609–616.
[36] J. Benítez, L. Becco, I. Correia, S. Milena Leal, H. Guiset, J. Costa Pessoa, J. Lorenzo, S. Tanco, P. Escobar, V. Moreno, B. Garat, D. Gambino, J. Inorg. Biochem. 105 (2011) 303–311.
[37] J. Benítez, A. Cavalcanti de Queiroz, I. Correia, M. Amaral Alves, M.S. Alexandre-Moreira, E.J. Barreiro, L. Moreira Lima, J. Varela, M. González, H. Cerecetto, V. Moreno, J. Costa Pessoa, D. Gambino, Eur. J. Med. Chem. 62 (2013) 20–27.
[38] M. Fernández, J. Varela, I. Correia, E. Birriel, J. Castiglioni, V. Moreno, J. Costa Pessoa, H. Cerecetto, M. González, D. Gambino, Dalton Trans. 42 (2013) 11900–11911.
[39] K. Wüthrich, Helv. Chim. Acta 48 (1965) 1012–1017.
[40] N.D. Chasteen, in: J. Reuben (Ed.), Biological Magnetic Resonance, Plenum, New York 1981, pp. 53–119.
[41] J. Costa Pessoa, T. Gajda, R.D. Gillard, T. Kiss, S.M. Luz, J.J.G. Moura, I. Tomaz, J.P. Telo, I. Torok, J. Chem. Soc. Dalton Trans. (1998) 3587–3600.
[42] T.S. Smith, R. Lobrutto, V.L. Pecoraro, Coord. Chem. Rev. 228 (2002) 1–18.
[43] G. Micera, V.L. Pecoraro, E. Garribba, Inorg. Chem. 48 (2009) 5790–5796.
[44] J. Costa Pessoa, S. Marção, I. Correia, G. Gonçalves, A. Dornyei, T. Kiss, T. Jakusch, I. Tomaz, M.M.C.A. Castro, C.F.G.C. Geraldes, F. Avecilla, Eur. J. Inorg. Chem. (2006) 3595–3606.
[45] M.R. Maurya, A.A. Khan, A. Azam, A. Kumar, S. Ranjan, N. Mondal, J. Costa Pessoa, Eur. J. Inorg. Chem. (2009) 5377–5390.
[46] M.R. Maurya, A.A. Khan, A. Azam, S. Ranjan, N. Mondal, A. Kumar, F. Avecilla, J. Costa Pessoa, Dalton Trans. 39 (2010) 1345–1360.
[47] M.R. Maurya, C. Haldar, A. Kumar, M.L. Kuznetsov, F. Avecilla, J. Costa Pessoa, Dalton Trans. 42 (2013) 11941–11962.
[48] S.P. Dash, S. Majumder, A. Banerjee, M.F.N.N. Carvalho, P. Adão, J. Costa Pessoa, K. Brzezinski, E. Garribba, H. Reuter, R. Dinda, Inorg. Chem. 55 (2016) 1165–1182.
[49] M.R. Maurya, N. Chaudhary, F. Avecilla, P. Adão, J. Costa Pessoa, Dalton Trans. 44 (2015) 1211–1232.
[50] A. Levina, A. Mitra, P.A. Lay, Metallomics 1 (2009) 458–470.
[51] C. Gruning, D. Rehder, J. Inorg. Biochem. 80 (2000) 185–189.
[52] I. Correia, S. Marção, K. Koci, I. Tomaz, P. Adão, T. Kiss, T. Jakusch, F. Avecilla, J. Costa Pessoa, Eur. J. Inorg. Chem. 694-708 (2011).
[53] G. Fotakis, J.A. Timbrell, Toxicol. Lett. 160 (2006) 171–177.
[54] E. Vega-Avila, M.K. Pugsley, Proc. West. Pharmacol. Soc. 54 (2011) 10–14.

[55] E. Rodríguez Arce, C. Sarniguet, T.S. Moraes, M. Vieites, A.I. Tomza, A. Medeiros, M.A. Comini, J. Varela, H. Cerecetto, M. González, F. Marques, M.H. García, L. Otero, D. Gambino, J. Coord. Chem. 68 (2015) 2923–2937.

[56] T.S. Morais, T.J.L. Silva, F. Marques, M.P. Robalo, F. Avecilla, P.J. Amorim Madeira, P.J.G. Mendes, I. Santos, M.H. Garcia, J. Inorg. Biochem. 114 (2012) 65–74.

[57] H. Faneca, V.A. Figueiredo, A.I. Tomaz, G. Gonçalves, F. Avecilla, M.C. Pedroso de Lima, C.F.G.C. Geraldes, J. Costa Pessoa, M.M.C.A. Castro, J. Inorg. Biochem. 103 (2009) 601–608.

[58] L. Vilas Boas, J. Costa Pessoa, Vanadium, in: G. Wilkinson, R.D. Gillard, J.A. McCleverty (Eds.), Comprehensive Coordination Chemistry, vol. 3, Pergamon, Oxford 1987, pp. 453–583.

[59] L. Naso, M. Valcarcel, P. Villacé, M. Roura-Ferrer, C. Salado, E.G. Ferrer, P.A.M. Williams, New J. Chem. 38 (2014) 2414–2421.

[60] L. Naso, E.G. Ferrer, L. Lezama, T. Rojo, S.B. Etcheverry, P. Williams, J. Biol. Inorg. Chem. 15 (2010) 889–902.

[61] E.G. Ferrer, M.V. Salinas, M.J. Correa, L. Naso, D.A. Barrio, S.B. Etcheverry, L. Lezama, T. Rojo, P.A.M. Williams, J. Biol. Inorg. Chem. 11 (2006) 791–801.

[62] M.W. Makinen, M. Salehitazangi, Coord. Chem. Rev. 279 (2014) 1–22 (& refs. therein).

[63] D. Wyrzykowski, I. Inkielewicz-Stępniak, J. Pranczk, K. Żamojć, P. Zięba, A. Tesmar, D. Jacewicz, T. Ossowski, L. Chmurzyński, Biometals 28 (2015) 307–320.

[64] W. Malorni, F. Iosi, F. Mirabelli, G. Bellomo, Chem. Biol. Interact. 80 (1991) 217–236.

[65] A.P. Matos, F. Marques, P. Ingram, in: A. Méndez-Vilas (Ed.), Microscopy: Advances in Scientific Research and Education 2014, pp. 32–38.

[66] L. Côrte-Real, A.P. Matos, I. Alho, T.S. Morais, A.I. Tomaz, M.H. Garcia, I. Santos, M.P. Bicho, F. Marques, Microsc. Microanal. 19 (2013) 1122–1130 (and herein ref 25).

[67] E. Fuchs, D.W. Cleveland, Science 279 (1998) 514–519.

[68] H. Lodish, A. Berk, S.L. Zipursky, P. Matsudaira, D. Baltimore, J. Darnell, Molecular Cell Biology, fourth ed. W. H. Freeman, New York, 2000.